Behavior And Analysis Of The 10m Geodesic Dome For Class I And II Subdivision For Breakdown Methods 1 And 2 Under Lateral Load

Ms. Komal B. Lendave[1], Assistant Prof. P.V. Dhanshetti [2], Dr. S. S. Patil[3]

Abstract

Historically, practically all blocky constructions had roofs supported by column timbers. Although the columns prevented the heavy roofs from collapsing, they provided very little open internal space. The gravestone was used to construct the uppermost domes. Domes became taller as they became heavier. In the 1950s, architects saw domes differently for the first time, thanks to a revolutionary new design known as "The Geodesic Dome". The spherical shape of a dome enables for unfettered air and energy circulation, making it one of the most efficient interior conditions for mortal homes. The exploratory paper for class I and II subdivisions compare geodesic domes with 10m dome radius. Breakdown systems 1 and 2, also known as class I system 1 and class I system 2, use 4v, 6v, 8v, 10v, and 12v dome frequencies, respectively. CADRE GEO 7.0 developed the dome model. STAAD Pro software is used to carry out the analysis.

Keywords *Geodesic Dome, Dome Frequency, Load Distribution, Breakdown Method, Triangular Elements.*

1. Introduction

A geodesic dome is a spectacular architectural building defined by its spherical or hemispherical shape and is made up of a network of interconnected triangles. R. Buckminster Fuller, an architect and engineer,[1] popularized the unique design of the geodesic dome, which is known for its structural efficiency and versatility. Geodesic domes are sturdy and stable due to their geometry, which evenly distributes strain and stress.

Geodesic domes are cost-effective and environmentally benign due to their capacity to enclose enormous interior spaces with minimum resources. Because of their robustness and adaptability, they have found a wide range of applications, including housing and event spaces, greenhouses, and aerospace.

Geodesic domes are a symbol of architectural innovation because of their unique look and futuristic design. A geodesic dome is used for shelter, recreation, or scientific inquiry. Geodesic domes, which demonstrate the creativity of structural engineering and design, represent a harmonious balance of form and function.

---

[1] PG Student, Civil Engineering Department, Walchand Institute of Technology, Solapur, Maharashtra, India

[2] Assistant Professor, Civil Engineering Department, Walchand Institute of Technology, Solapur, Maharashtra, India

[3] Professor, Civil Engineering Department, Walchand Institute of Technology, Solapur, Maharashtra, India

[1] Address: Block no. 30, Mohite Nagar, Hotgi Road, Solapur 413003

[2] Address: Plot No. 72, Rutu Vihar near Jagdamba Nagar, Jule Solapur, Solapur 413224

[3] Address: Plot no. 109 Bhagyashree Niva, Veershaiva Nagar, near Mehta School, Vijapur Road, Jule Solapur 413004

2. Literature Review

2.1 Ana T. V. et al. (2015)

This study investigates the relationship between a big concrete monolithic dome's diameter, rib count, and compressive strength. Domes have been used to construct silos, residential buildings, schools, stadiums, industrial roofs, nuclear reactors, pressure vessels, auditoriums, and stadiums because they provide a safe environment, use little material, are simple to erect, are efficient at retaining heat, and have a membrane action. The finite element study shows that when the diameter of the dome increases from 70 to 100 meters, the ultimate load capacity increases by roughly 32.5%. The reduction in dome diameter from 70 meters to 50 meters results in a 31.2% reduced final load capacity. When concrete with a compressive strength of 30 MPa is increased to 35 MPa, its ultimate load capacity improves by 10%. Concrete's ultimate load capacity decreases by 8% when its fck value is 25 MPa rather than 30 MPa. The maximum load capacity of the dome improves by approximately 25% when four axisymmetric meridional ribs are used instead of two. The removal of the dome's two original meridional ribs lowered the total load capacity by 21.2%.

2.2 Devish G. Mandali and Associates (2016)

A geodesic dome with a diameter of 20 meters was used to compare Class I subdivision and breakdown procedures 1 and 2, also known as Class I procedures 1 and II, which are both used for 4V, 6V, 8V, 10V, and 12V dome frequencies in terms of live, dead, and wind loads. The dome's model was created using the CADRE Geo 7.0 software. STAAD Pro handles both analysis and design. The STAAD optimization tool is used for the optimization process. Their investigation led them to the conclusion that bottom rings gathered together have the most compressive axial force. In terms of compressive axial force, the lower four rings, for example, are labeled as RING 1, RING 2, RING 3, RING 4, and RING 5 and are grouped separately. A TOP-PENTAGON consists of five people positioned from the crown to the RING. The remaining bottom diagonal members between horizontal rings are referred to as BOTTOM.

After optimizing the model using both strength and deflection requirements, each component will have unique sectional characteristics. They determined the dome's self-weight by grouping the rings and performing an empirical computation. The empirical formula for Class I Method I is T = 4.0611f4 - 48.348f3 + 195.78f2 - 292.5f + 358.38, while for Class I Method II it is T = 0.7567f4 - 8.8494f3 + 39.714f2 - 66.691f + 273.4. The tonnage (KN) increases for both breakdown procedures as the dome frequency increases (where T is the quantity in tons and f is the frequency); nevertheless, the empirical formula shows that method 2's 8v dome frequency reduced the tonnage by 5.013%. Member sizes shrink, whereas tonnage for Class I Method 2 increases in lockstep with growing dome frequency. They decided that Class I method 1 division is the optimum option for frequencies 4 and 8 volts. Class I method 2 division is the preferred approach for achieving maximum tonnage.

2.3 Lakhov A. (2017)

Problems with the classification of geodesic shells and domes are addressed in this work. The present taxonomy of geodesic shells and domes is discussed in this article along with its shortcomings. This category is limited to geodesic domes with a single contour plate. To address the shortcomings of geodesic shell schemes, they devised a logical classification system. For the logical classification of geodesic domes, they chose specific attributes. The geodesic domes and shells were organized in a reasonable manner. It introduced a vocabulary

for creating geometrical geodesic shell models and included examples of various geodesic shell kinds. The logical classification for a single contour yields 48 geodesic dome types. New parametric ArchiCAD elements have been added to the GEODOME collection. This page explains the various classification systems. The geodesic shells and domes are catalogued on paper. There are currently automatic classifications based on cutting-edge information technology. The electronic document can be exhibited to bring the objects, events, and processes being studied to life. An interactive computerized classification of a geodesic shell and dome was developed. The user interface of an electronic geodesic dome classification program is centered on buttons that display geodesic shell classes and subclasses. The geodesic shell and dome classification system facilitates forecasting, data organization, and information dissemination.

2.4 Gaurav, V. G. & colleagues (2021)

Domes can fail for a variety of causes and take many different forms. This project covers the design and study of a monolithic dome sub-structured like an auditorium. Their design allows them to load evenly across the plates. This project will use STAAD-Pro to evaluate and design the concrete dome structure, as well as apply point loads to the nodal joints. This study models the column height and dome at different spans. Each model depicts the displacement, responses, beam forces, shear stress, membrane stress, primary stress, von Mis stress, and tau stress. When compared to the other models, model no-V produces the best displacement results.

2.5 Abhas Shrivastava et al. (2021)

In this article, three alternative cross-sectional shapes (rectangular, square, and circular) are allocated to the components of an icosahedron geodesic dome in order to detect stress fluctuations. Geodesic domes are substantially more significant in terms of force distribution since an icosahedron is made up of triangles and forces are distributed equally over the shape. This is because a triangle's base absorbs all of the force applied to its corner. The goal of the research is to identify the cross-sectional form that will allow for greater dome member optimization at lower stress values. The geodesic dome models are created using the application CADRE GEO 7.0. The analysis is performed using the STAAD.PRO V8i SS6 program. The researchers determined that circular tubular sectional designs produce the highest stress values, whereas square hollow tubular sectional shapes produce the lowest stress levels. This led them to the conclusion that round hollow tubes may be made less expensive and have a lower deadweight by utilizing a component with a smaller cross-section.

2.6 Findings from the literature review and comparison with previous research studies

According to the literature on geodesic domes mentioned above, researchers have investigated the tonnage of the dome for class I and class II subdivision, which section size is more efficient for the structure of the dome, and which dome is more practical in use.

Table 1 Comparison with previous research studies

Study	Highlighted Method or Type	Technique in study	Result

Aabhas Shrivastava et al. [5]	Class I Subdivision for Breakdown Method 1 has a radius of 12, 18, 24, and 30 meters and dome frequencies of 2 v, 4 v, 6 v, 8 v, and 10 v.	The STAAD Pro application is used to provide dome members three various cross-sectional shapes—rectangular, square, and circular—in order to look for stress changes. They used STAAD Pro to divide rings into DL, LL, and WL categories.	Square hollow tubular sectional shapes have the highest stress values. The minimal stress value is calculated for a circular tubular shape. Finally, a lower cross-section member for circular hollow tubular could be used, lowering the structure's dead weight and making it more cost-effective.
Divyesh G. et al. [3]			They compared the tonnages, or structure weights, of Class I Method 2 and Class I Method 1 domes at four different voltages: four, six, eight, ten, and twelve volts. Their research revealed that when dome frequency increases, so does tonnage (KN).
Kunjan Bharwad et al. [4]	Class I subsection concerning procedures of breakdown Geodesic domes with a 20m diameter and frequencies of 4v, 6v, and 8v are classified into two categories.	ANSYS Workbench is used to optimize a 20-meter-diameter geodesic steel dome at various frequencies. Geometry for the geodesic dome is created with the CADRE Geo software, loaded into STAAD Pro, and then imported into the ANSYS workbench via Java scripting. The response surface optimization toolbox is used to reduce the overall weight of the dome while accounting for a variety of constraints,	They determined that the ideal weight found in the ANSYS workbench outperforms and is more reliable than earlier investigations. The response surface optimization toolbox is useful for experimenting with alternative frequencies, division methods, and diameters since it delivers better optimization results than other tools. It also helps to optimize other structures.

		including stresses and deflection.	
Gaurav Vijay Ghugare et al. [6]	This project includes the design and study of a monolithic dome with an auditorium substructure. The models in this project are suitable for columns with a diameter of 7 meters, 15 meters, 16 meters, 17 meters, 18 meters, and 22 meters.	Their aim is to give even loading throughout the plate. STAAD Pro will be utilized to conduct applied point load analysis and design of the concrete dome structure over the nodal joints.	This work simulates the dome at various spans up to the column's height. It is revealed that forces and tensions grow as the model's height increases. Stresses are shown to grow as the models' span increases.

After reading this study report, I concluded that more research in a geodesic dome is required to establish which class subdivision and breakdown method are most suited for various load applications. Specifically, I feel that an analysis of geodesic domes for class I and class II subdivisions using breakdown methods 1 and 2 for changing dome diameters and dome frequencies is currently absent. This work focuses on the behavior and analysis of geodesic domes under lateral stress in class I and class II subdivisions with a dome diameter of 10m, utilizing breakdown methods 1 and 2.

2.7 Scope of work

The scope includes a thorough examination into the behavior and response of the geodesic dome under lateral load for various subdivision classes using breakdown methods.

1. The dome measures 10m and is commonly used for indoor stadiums and banquettes.

2. The dome is designed for both class I and II.

3. The study covers breakdown methods 1 and 2 for both classes (Class I method 1, Class I method 2, Class II method 1, and Class II method 2).

4. Evaluate dome response to lateral loads, including seismic, wind, and gravity loads.

5. Evaluate different factors, including node displacements, shear force, bending moments, support reactions, support moments, and beam displacement.

6. Identify the appropriate dome structure for a 10 m radius.

3. Methods

There are several methods for building geodesic domes, depending on how the triangles are organized and the type of dome being built.

1. A 10 m radius dome was modeled and analyzed using class I and breakdown methods 1 and 2 for frequencies of 4v, 6v, 8v, 10v, and 12v.

2. We modeled and analyzed a 10 m radius dome for class II, using breakdown methods 1 and 2 for frequencies of 4v, 6v, 8v, 10v, and 12v.

3. Lateral seismic stress is applied according to IS 1893-2016.

4. Wind load is imposed based to IS 875 (P-3) 2015.

5. Load combination is based on the Indian standard IS 800-2007.

STAAD Pro software was utilized for the examination of these domes. Cadre Geo Software was used for modelling.

3.1 Geodesic dome subdivision

Subdividing a geodesic dome is the process of breaking it down into smaller, easier-to-manage portions. This is done for a multitude of reasons, including as creating more space, improving insulation, or meeting certain architectural standards. Here are some popular approaches for dividing a geodesic dome:

3.1.1 Class I subdivision

A geodesic dome can be broken into smaller, more manageable portions, commonly triangles or other geometric shapes, using a technique known as Class subdivision. This subdivision is crucial for constructing the dome's supporting structure and covering. The simplest type of subdivision, known as Class I subdivisions, entails dividing the dome's faces into identical triangles. This technique simplifies construction and allows for the efficient use of resources, resulting in structural stability and homogeneous stress distribution throughout the structure.
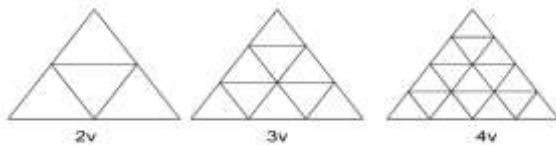

Figure 1 Class I Subdivision

3.1.2 Class II subdivision

Geodesic domes can be dissected into several polygons using the Class II approach. Typically, the various shapes are created by using triangles, pentagons, and hexagons. A Class II subdivision allows for a more elaborate and varied pattern on the dome's surface than a Class I subdivision, which requires all sides to be comparable triangles.
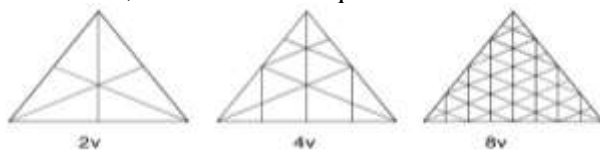

Figure 2 Class II Subdivision

3.1.3 Class III subdivision

A geodesic dome's surface is divided in the most elaborate and thorough way in a Class III subdivision. This type of subdivision divides the dome's faces into a variety of unique and complicated polygonal shapes. A Class III subdivision is typically designed to embellish the dome's surface with highly elaborate and creative patterns or decorations, making it visually appealing and architecturally distinctive.

3.2 Dome frequency

The triangulation method is called as frequency, and each line of the main polygon is divided into many segments. In shorthand, a number with the prefix "v" represents frequency. The shape of a 1-frequency dome, or "1v," is created by laying an icosahedron on the ground with its bottommost section removed. In a 1V dome, each strut has the same segment. Then, using a technique known as "tessellation," we will divide each triangle segment of the 1v dome into smaller triangle parts. Tessellation creates a larger dome with shorter segments, making the dome more globular and increasing the frequency of geodesic domes. Tessellation divides the triangular face of an icosahedron into smaller triangles, increasing the frequency of the geodesic dome.
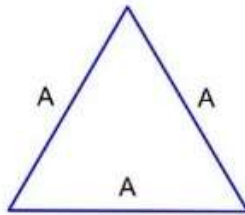
Figure 3 1v Triangle with no tessellation

3.3 Defining loads

The loads evaluated in the analysis include earthquake, wind, movement, and dead loads. Wind load is the primary determining factor for dome-shaped structures. Wind loads are calculated in accordance with IS 875 (part 3)-2015. IS 800 specifies the usage of load combinations.
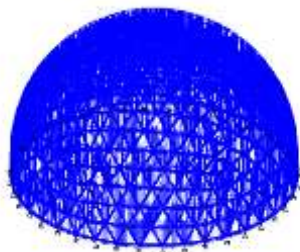
Figure 4 Live Load

Table 2 Parameters for the wind

Fundamental wind speed (m/sec)	55
Category	I
Risk coefficient / Probability factor	1

Topography factor	1
A cyclonic region's importance factor	1
Wind directionality factor (m/sec)	1
The area averaging factor	0.9
The combination factor	1

Table 3 Height Vs. Intensity of Wind Pressure

H	k2	$(Pz = 0.6 * Vz^2)$	P (KN/m^2)	0.7*Pz (KN/m^2)	Pd max of 0.7*Pz & P (KN/m^2)
10	1.05	2001.04	1.80	1.401	1.801
15	1.09	2156.40	1.94	1.509	1.941
20	1.12	2276.73	2.05	1.594	2.049

H= height of building in m,
K2= Terrain & height multiplier for Terrian category-1
Pz = wind pressure,
Vz = design wind speed at height z.
Pd = design wind pressure
The STAAD Pro application uses the above-mentioned data to determine wind loads. The external pressure co-efficient (Cpe) for curved roofs is calculated using clause 7.3.3.6 and table no. 18 of IS 875 (part 3) 2015. For H/L = 0.5, the wind-ward and lee-ward factors are 1.2 and 0.7, respectively.
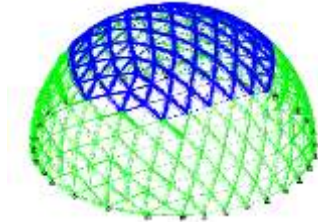
Figure 5 Wind Load

The following parameters are considered for seismic analysis

Table 4 Seismological Parameters

Parameters	Values
Zone	0.36
Response reduction factor (RF)	5
Importance factor (I)	1
Rock & soil site factor (SS)	1
Type of structure (ST)	1
Damping ratio (DM)	0.02

3.4 Load combinations

The load combination is as per IS 800-2007. The following load combinations were studied.
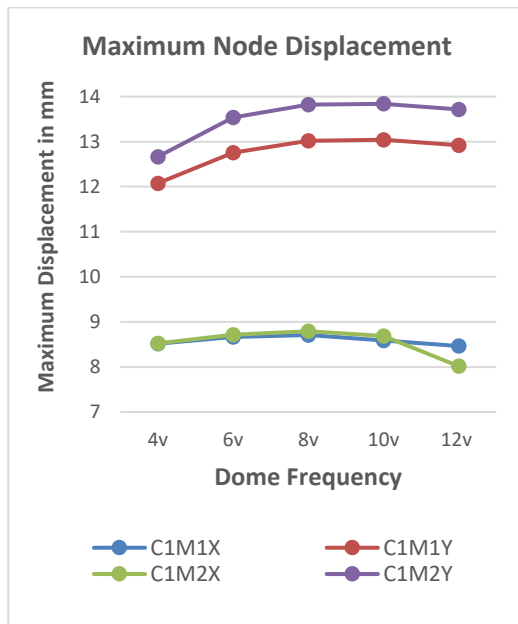
1) 1.5 (DL + LL)
2) 1.2 (DL + LL + WL)
3) 1.5 (DL + WL)
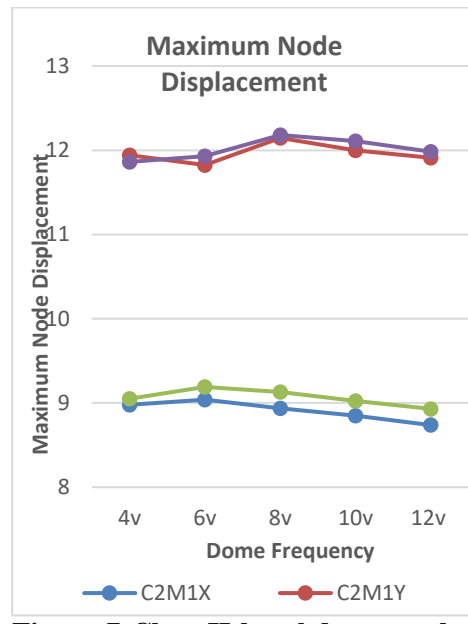4) 1.2 (DL + LL + EL)
5) 1.5 (DL + EL)

4. Results

C1 and C2 = Class I & Class II
M1 and M2 = Method1 & Method II

4.1 Nodal Displacement

Figure 6 Class I breakdown methods 1 & 2
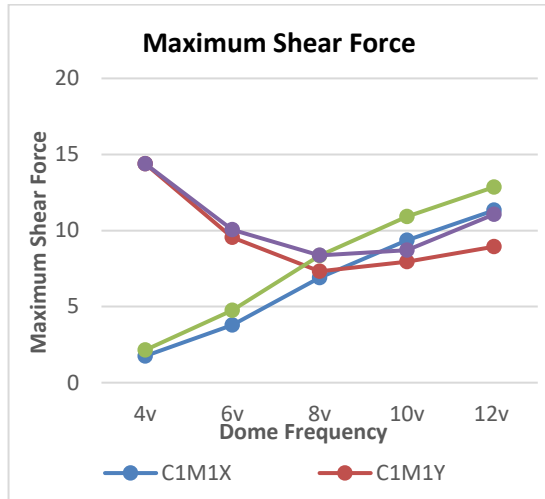
Figure 7 Class II breakdown methods 1 & 2

It has been observed that when dome frequency increases, nodal displacement rises from 4v to 8v before decreasing. Figure 6 shows the maximum displacement for Class I breakdown methods 1 and 2, whereas Figure 7 shows Class II breakdown methods 1 and 2.

For both approaches (approaches 1 and 2), Class I exhibits more displacement than Class II. The study found that method 1 increased displacement by 13.61% when compared to class II method 1, and method 2 increased displacement by 4.52% when compared to class II method 2.

For class I, method 1 increases nodal displacement by 57.40% and 48.34% in the X and Y directions, respectively, as compared to method 2. For class II method 1, nodal displacement increases by 34.76% in the X direction and 32.55% in the Y direction when compared to method 2 for the same class.

4.2 Shear Force

Shear force and bending moment are significant aspects to consider. The maximum shear force for classes I and II using breakdown techniques 1 and 2 is as follows.

Figure 8 Maximum Shear Force for Class I breakdown methods 1 & 2
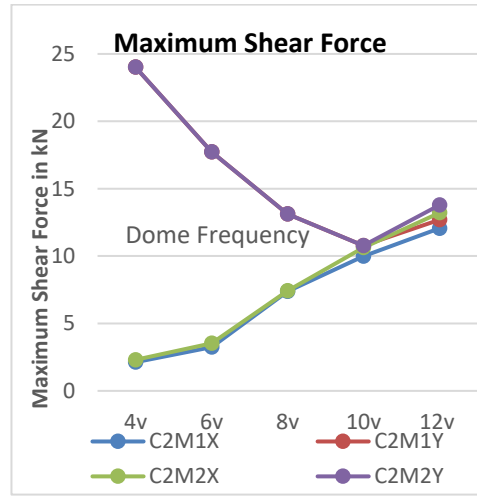
Figure 9 Maximum shear force class II breakdown methods 1 & 2

The shear force for class I is larger than class II. The Shear Force in the X direction for both classes and methods increases as the dome frequencies increase. In the Y direction for class, Shear Force decreases until 8V, then increases. technique I and technique 2 had a 49.16% and 41.89% drop in SF, respectively, compared to 4V. In the Y direction, Shear Force reduces up to 10V before increasing. SF decreases by 55.11% for both techniques.

4.3 Bending Moment

The bending moment is another significant issue. The bending moment for class I and class II in breakdown method 1 and 2 are
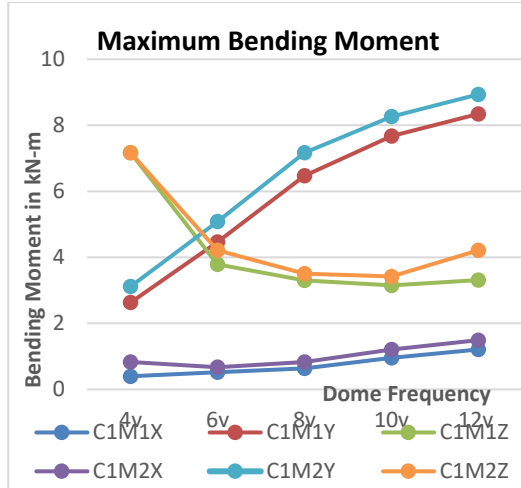
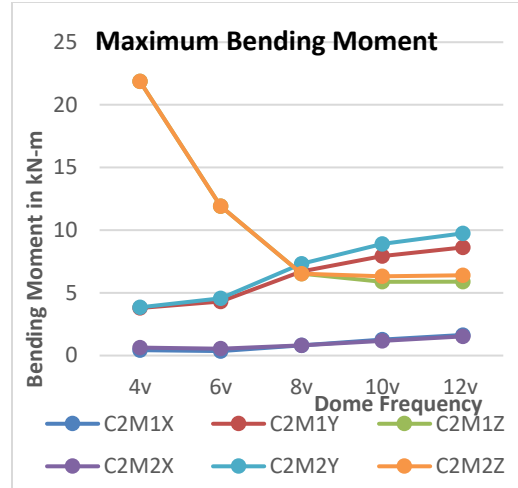**Figure 10 Bending moment for class I breakdown method I & II**

Figure 11 Bending moment class II breakdown method I & II

The bending moment for class II is 22.45% and 25.12% higher than that of class I in the X and Z directions, respectively. However, the bending moment continues to increase in the Y direction.

The bending moment increases in the X and Y directions for both classes and techniques as the dome frequency increases. In the Z direction, it gradually decreases until it reaches 10V for both classes and methods before increasing. The percentage reduction is 52.27% for class I and 71.09% for class II.

4.4 Reaction at support

The maximum reaction and maximum bending moment at support for breakdown techniques I and II of class I subdivision are:
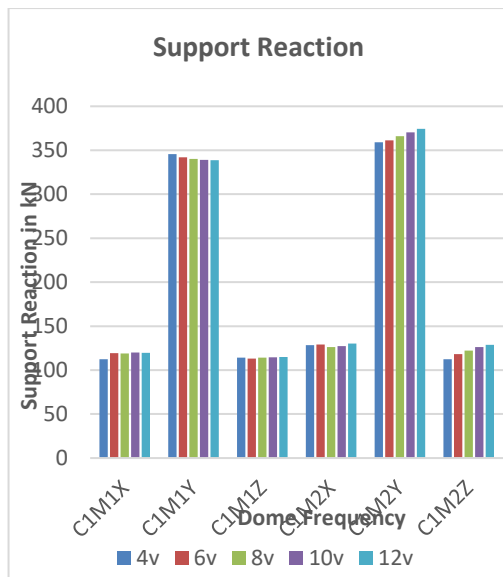
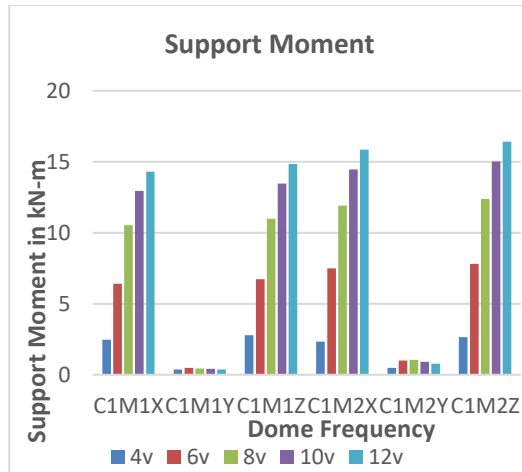**Figure 12 Maximum support reaction class I breakdown method I & II**
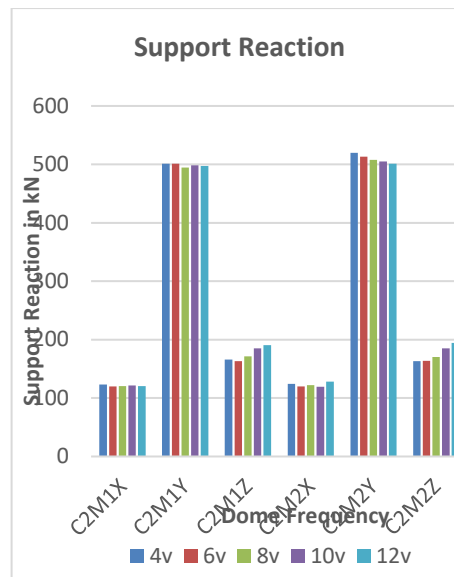
Figure 13 Maximum support reaction class II breakdown method I & II

Both techniques show that support reactions are lower for the Class I subdivision than for Class II.

The reactions are found to be greater in the Y direction for both classes, but for class I method 1, the reactions decrease somewhat with an increase in dome frequencies, whereas for class I method 2, the reactions increase slightly with an increase in dome frequencies.

In the Y direction, for class II method 1, the support reactions are found to be the smallest for 8v dome frequency compared to others, however for class II method 2, they continue to decrease as dome frequencies increase.

4.5 Moment at support

**Figure 14 Maximum support moment for Class I breakdown method I & II**
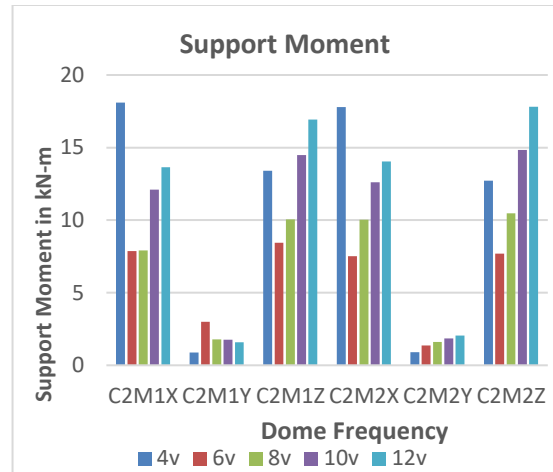
Figure 15 Maximum support moment for Class II breakdown method I & II

For both classes of methods 1 and 2, the support moments are much higher in the X and Z directions than in the Y directions. Class II has somewhat higher support moments than class I, which is 10.18% higher. For class I, procedure 1 and 2, the support moment increases as the dome frequency increases. For class II for method 1 and 2, the support moments are least for 6v and maximum for 4v, which is 2.3 times more than 6v.

4.6 Axial force
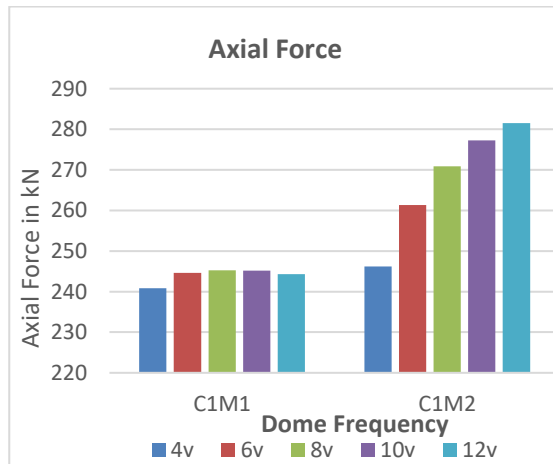
Figure 16 Axial force for Class I breakdown method I & II
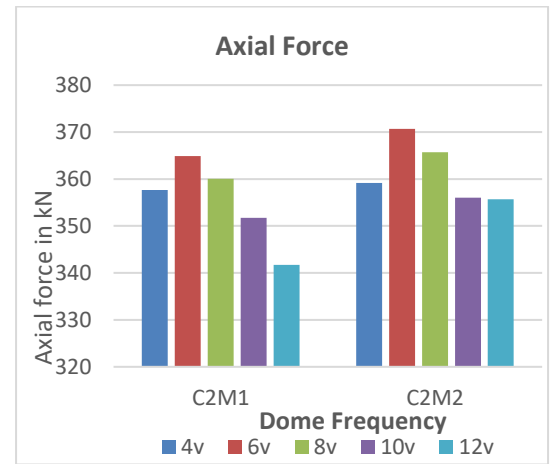
Figure 17 Axial force for Class II breakdown method I & II

The axial forces in class II for both procedures are 31.67 percent stronger than in class I.

Method 2 has axial forces that are 12.88% more than method 1 for class I, and the axial forces for method 2 continue to increase as dome frequencies increase.

The axial forces for class II method 1 continue to drop as dome frequencies grow, whereas for method 2, they are highest at 6v, decrease to 10v, and remain almost constant as dome frequencies climb.

5. Discussion

1. The weight of the structure increases with dome frequency for classes I and II, regardless of the breakdown mechanism. Due to the shorter strut length in class I, there are more beams observed than in class II.

2. For all dome frequencies, class I, class II, and breakdown procedures, the largest nodal displacement occurs at the top. Class I has more displacements than class II for both procedures 1 and 2, by 13.61 and 4.52 percent, respectively. Method 1 has a higher nodal displacement than Method 2 in both classes.

3. Class I exhibits larger shear forces compared to class II in both techniques 1 and 2. The shear force for technique 2 in both classes increases as the dome frequencies increase. Shear force for method 1 drops from 4v to 8v and 10v, then increases for class I and class II, respectively.

4. Class II has larger bending moments (22.45 to 25.12 percent) in X and Z directions compared to class I. Bending moment increases with dome frequency in the X and Y directions, but decreases in the Z direction for 8v and 10v for classes I and II, respectively.

5. Support reactions are lower in the Class I subdivision compared to Class II for both techniques. Both classes show larger reflexes in the Y direction. Class II has a somewhat higher support moment (10.18%) than class I.

6. Class II technique 1 has diminishing axial forces as dome frequencies increase, but method 2 has a maximum at 6v, reduces up to 10v, and remains almost constant with higher dome frequencies. For both approaches, axial forces for class II are determined to be 31.67 percent more than for class I.

6. Conclusion and Future research scope

Class II subdivision is more complicated than class I subdivision. Breakdown Method 1 provides a quick summary, but Breakdown Method 2 provides a more detailed and precise depiction. Class II subdivision using Breakdown Method 2 provides a more realistic picture of the geodesic dome's behavior, despite the fact that it requires more analysis and processing time. Material characteristics, loadings, and safety considerations must all be carefully considered for a thorough and reliable analysis.
Future research in geodesic domes:
1. Analyzing the behavior and breakdown procedures of a double-layer geodesic dome.
2. Due to its intricate geometry, Class III sub-division requires in-depth study.
3. Analyzing the behavior of a geodesic dome with a column, which is not directly placed in the ground and experiences varying lateral loads.
4. Research and planning for the geodesic dome chimney at the top.

Acknowledgments

References
1. Ansa T Varghese, Manju George, "Study on the effect of Diameter, Compressive Strength and Number of Ribs on the Large Concrete Monolithic Dome" International Journal of Engineering Development and Research (IJEDR), Volume 3, Issue 4, ISSN: 2321-9939, 2015, pp. 300-303.
2. Riya Anna Abraham, G. Kesava Chandran, "Study of Dome structures with specific Focus on Monolithic and Geodesic Domes for Housing" International Journal of Emerging Technology

and Advanced Engineering (IJETAE), Volume 6, Issue 08, ISSN: 2250-2459, August 2016, pp. 173-182.

3. Divyesh G. Mandali, Satyen D. Ramani, "Comparative study for geodesic dome of Class I subdivisions", Journal of Emerging Technologies and Innovative Research (JETIR), Volume 3, Issue 5, ISSN: 2349-5162, May 2016, pp. 165-171.

4. Kunjan Bharwad, Satyen Ramani, "Structural Optimization of Class2(Method2) Type Geodesic Steel Dome Using ANSYS® Workbench", Journal of Emerging Technologies and Innovative Research (JETIR), Volume 4, Issue 04, ISSN-2349-5162, April 2017, pp. 341-349.

5. Aabhas Shrivastava, Umesh Pendharkar, "Study of Optimized Sectional Shape for Geodesic Domes" Journal of Xi'an University of Architecture & Technology, Volume 13, Issue 01, ISSN: 1006-7930, 2021, pp. 407- 411.

6. Gaurav Vijay Ghugare, Prof. Vishal Sapate, "Structural Analysis of Dome Structure by STAAD Pro" International Journal for Research in Applied Science & Engineering Technology (IJRASET), Volume 9 Issue 4, ISSN: 2321-9653, April 2021, pp. 1515-1520.

7. Tien T. Lan, "handbook of Structural Engineering", Institute of Building Structures, MChinese Academy of Building Research, Second Edition, CRC Press 1997.

8. M.Kooshkbaghi et.al, "Optimal geometry design of single layer lamella domes using charged system search algorithm", J. Appl. Environ. Biol. Sci., Volume 5(12S)846-854, ISSN: 2090-4274, 2015, pp. 846-854.

9. H. Tagawa and M. Oshaki, "A continuous Topology Transition Model for Shape Optimization of Plane Trusses with uniform cross-sectional area", third world congress of structural and multidisciplinary optimization (Buffalo, New York, 1999), pp. 1-6.

10. O. Hasancebi, F. Erbatur, "Layout optimization of trusses using simulated annealing", In Proc: 5th International Conference on Computational Structure Technology, Computational Engineering using metaphors from nature (Topping, B.H.V., ed.) (Elsevier, Leuven. pp.175-190, 2000)

11. X. Guo and G. Cheng, "E-Continuation approach for truss topology optimization", Third World Congress of Structural and Multidisciplinary Optimization (Buffalo, New York, 1999), pp. 1-6.

12. Kaveh, A., and Shojaee, S. "Optimal design of skeletal structures using ant colony optimization." International Journal for Numerical Methods in Engineering, Volume 70, Issue 5, October 2006, pp. 563–581.

13. Camp, C. and Bichon, B. "Design of Space Trusses Using Ant Colony Optimization." Journal of Structural Engineering, (ASCE), Volume 131, Issue 3, ISSN:0733-9445, 2004, pp. 741-751.

14. M. Serra and Venini P. "On some applications of ant colony optimization metaheuristic to plane truss optimization", Struct Multidisc Optim (2006) 32 DOI 10.1007/s00158-006-0042-x, February 2006, pp. 499–506.

15. Saka MP, "Optimum geometry design of geodesic domes using harmony search algorithm", Advances in Structural Engineering, Volume 10, Issue 6, December 2007, pp. 595-606.

16. LRFD-AISC, "Manual of Steel Construction, Load and Resistance factor design", Metric conversion of the second edition, Chicago: AISC. vols. 1 & 2, 1999.

17. A. Kaveh, S. Talatahari, "Optimal design of Schwedler and ribbed domes via hybrid big bang-bid crunch algorithm", Journal of Constructal steel research, Volume 66, Issue 3, ISSN: 1873-5983, March 2010, pp. 412-419.

18. A. Kaveh, S. Talatahari, "Optimal design of single layer domes using meta-heuristic algorithms, a comparative study", International Journal of Space Structure, Volume 25, ISSN: 0266-3511, 2010, pp.217-227.

19. M. P. Saka, E. S. Kameshki, "Optimum design of nonlinear elastic framed domes", Advances in Engineering Software, Volume 29, Issues 7-9, ISSN: 0965-9978, August – November 1998, pp. 519-528.

20. Hongyu Wu, Yu-Ching Wu, Peng Zhi, Xiao Wu, Tao Zhu, "Structural optimization of single–layer domes using surrogate–based physics – informed neural networks", Heliyon, Volume 9, Issue 10, e20867, October 2023, pp. 1-20.

21. Saeid Kazemzadeh Azad, Saman Aminbaksh, Samer S. S. Shaban, "Multi-Stage guided stochastic search for optimization and standardization of free–form steel double – layer grids", Structures, Volume 34, ISSN: 2352-0124, December 2021, pp. 678-699.
22. Pooya Zakian, "Metaheuristic design optimization of steel moment resisting frames subjected to natural frequency constraints", Advances in Engineering Software, Volume 135, ISSN: 1873-5339, September 2019, 102686.
23. O. Hasancebi, S. Carbas, E. Dogan, F. Erdal, M. P. Saka, "Performance evaluation of metaheuristic search techniques in the optimum design of real size pin jointed structures", Computers and Structures, Volume 87, Issue 5-6, ISSN: 1879-2243, March 2009, pp. 284-302.
24. Maggie Kociecki, Hojjat Adeli, "Shape optimization of free–form steel space–frame roof structures with complex geometries using evolutionary computing", Engineering Applications of Artificial Intelligence, Volume 38, ISSN: 1873-6769, February 2015, pp. 168-182.
25. Jose P. G. Carvalho, Afonso C. C. Lemonge, Patricia H. Hallak, Denis E. C. Vargas, "Simultaneous sizing, shape, and layout optimization and automatic member grouping of dome structures", Structures, Volume 28, ISSN: 2352-0124, December 2020, pp. 2188-2202.
26. S. O. Degertekin, l. Lamberti, I. B. Ugur, "Sizing, layout and topology design optimization of truss structures using the Jaya algorithm", Applied Soft Computing, Volume 70, ISSN: 1872-9681, September 2018, pp.903-928.
27. Fuat Erbatur, Oguzhan Hasancebi, Ilker Tutuncu, Hakan Kilic, "Optimal design of planer and space structures with genetic algorithms", Computers and Structures, Volume 75, Issue 2, ISSN: 1879-2243, March 2000, pp. 209-224.
28. A. Kaveh, Razaei M., "Optimal design of double-layer domes considering different mechanical systems via ECBO", Iran journal Science Technology Trans. Civil Engineering, Volume 42, ISSN: s40996-018-0123-2, 2018, pp. 333-344.
29. Eltayeb Elrayah Kralafalla, "Computer Added Processing Of Geodesic Structural Forms" A Thesis Submitted For The Degree Of Doctor Of Philosophy University Of Surrey Department Of Civil Engineering, August 1994.
30. Hugh Kenner "Geodesic math and how to use it", University of California Press Berkeley, Los Angeles, London.
31. Amal Sheik, Aneeta Anna Raju, "Feasibility study of Geodesic Dome as Disaster Resistant", International Research Journal of Engineering and Technology (IRJET), Volume 06, Issue 04, ISSN: 2395-0056, April 2019, pp. 4493-4495.
32. Laxmipriya S, Ragavi G, Sakthisree M., "The Concepts behind the Design of Geodesic Domes – An Overview" in Imperial Journal of Interdisciplinary Research (IJIR) Vol-3, Issue-3, 2017.
33. A. Sujatha, "Geodesic Domes and its Applications", Indian Journal of Science and Technology, Volume 7 (3S), Issue 5-6, ISSN: 0974-5645, March 2014, pp. 5-6.
34. Davis, T. (2011), Geodesic Dome, Pacific Domes, California.
35. Shah Yash Jayminkumar, Vaibhav Doshi, "A parametric study on steel dome structures", International Journal for Technological Research in Engineering, Volume 03, Issue 09, ISSN: 2347-4718, May 2016, pp. 2135-2138.
36. Xiuli Wang, Jiyun Chen, Chang Wu, (2008) "Dynamic analysis of single layer lattice shell with BRBs", 6th International Conference on Computation of Shell and Spatial Structures, Beijing University of Technology.
37. Raneem Al Azem, Wael Elleithy, Tech leong Lau, and Mohammed Parvez Anwar, "Parametric study of tensegrity structures under seismic loading", Web of Conferences 347, 03016, https://doi.org/10.1051/e3sconf/202234703016, 2022, pp. 1-12.
38. Fuller BR. Geodesic dome. United States Patent Office, patent 2, US2682235 A, 1959.

Declaration of interest statement

The author declares that they have no knowledge of any competing financial interests or personal ties that could have influenced the work disclosed in this paper.

Competing Interests

The authors have no relevant financial or non – financial interests to disclose.

Authors Contributions

First author contributed to the study conception and design. Material preparation, data collection and analysis were performed by Komal Babasaheb Lendave. The first draft of manuscript was written by Komal Babasaheb Lendave and all remaining author have review manuscript and approved the final manuscript.